Combinatorial effects of splice variants modulate function of Aiolos

Rosalia Caballero[1,2], Fernando Setien[1], Lidia Lopez-Serra[1], Manuel Boix-Chornet[1,3], Mario F. Fraga[1], Santiago Ropero[1], Diego Megias[4], Miguel Alaminos[5], Eva M. Sanchez-Tapia[2], Maria C. Montoya[4], Manel Esteller[1], Rogelio Gonzalez-Sarmiento[2,*] and Esteban Ballestar[1,*]

[1]Cancer Epigenetics Laboratory, Molecular Pathology Programme, Spanish National Cancer Research Centre (CNIO), Melchor Fernández Almagro 3, 28029 Madrid, Spain
[2]Molecular Medicine Unit-Department of Medicine, Center for Cancer Research (CIC), University of Salamanca, Salamanca, Spain
[3]Leukaemia Research Fund Centre at the Institute of Cancer Research, London, UK
[4]Confocal Microscopy and Cytometry Unit, Biotechnology Programme, Spanish National Cancer Research Centre (CNIO), Madrid, Spain
[5]Department of Histology (University of Granada) and Fundación Hospital Clínico, Granada, Spain
*Authors for correspondence (e-mails: gonzalez@usal.es; eballestar@cnio.es)

Accepted 26 May 2007
Journal of Cell Science 120, 2619-2630 Published by The Company of Biologists 2007
doi:10.1242/jcs.007344

Summary

The transcription factor Aiolos (also known as IKZF3), a member of the Ikaros family of zinc-finger proteins, plays an important role in the control of B lymphocyte differentiation and proliferation. Previously, multiple isoforms of Ikaros family members arising from differential splicing have been described and we now report a number of novel isoforms of Aiolos. It has been demonstrated that full-length Ikaros family isoforms localize to heterochromatin and that they can associate with complexes containing histone deacetylase (HDAC). In this study, for the first time we directly investigate the cellular localization of various Aiolos isoforms, their ability to heterodimerize with Ikaros and associate with HDAC-containing complexes, and the effects on histone modification and binding to putative targets. Our work demonstrates that the cellular activities of Aiolos isoforms are dependent on combinations of various functional domains arising from the differential splicing of mRNA transcripts. These data support the general principle that the function of an individual protein is modulated through alternative splicing, and highlight a number of potential implications for Aiolos in normal and aberrant lymphocyte function.

Key words: Aiolos, Chromatin, Epigenetics, Ikaros, Isoforms, Mi-2/NuRD

Introduction

Differentiation of hematopoietic progenitors in the lymphoid lineage, and the choice of effector function at later stages of this pathway depend on the tightly controlled activation and repression of a number of genes (Fisher, 2002). The precise coordination of these pathways is essential for the proper development of the immune system, and their deregulation plays an important role in the pathogenesis of hematopoietic malignancies.

A number of transcriptional regulators play a critical role at specific stages of T- and B-cell differentiation, presumably by regulating the expression of genes whose products affect the fate and function of lymphoid cells. The Ikaros family of proteins is a prime example of such factors (Georgopoulos et al., 1992). Early studies demonstrated that the proteins encoded by the Ikaros gene are essential for the proper development of the lymphoid arm of the hematopoietic system (Cortes et al., 1999). Subsequent studies with null and dominant-negative Ikaros mutants led to the identification of Aiolos (also known as IKZF3), Helios (IKZF2), Eos (IKZF4) and Pegasus (IKZF5) (Wang et al., 1998; Morgan et al., 1997; Honma et al., 1999; Perdomo et al., 2000).

Aiolos, the second Ikaros family member to be identified (Morgan et al., 1997), is particularly interesting for several reasons. Firstly, disruption of Aiolos leads to an increase in pre-B and immature B cells and to a severe reduction in circulating B cells (Wang et al., 1998). Moreover, Aiolos is also specifically required for the generation of long-lived, high-affinity plasma cells in the bone marrow, which are responsible for long-term immunity in humans (Cortes and Georgopoulos, 2004). In addition, Aiolos null mice display B-cell hyperproliferation and develop lymphomas, suggesting that this gene may have a role in tumor suppression (Wang et al., 1998). Furthermore, the elevated serum antibody levels and autoantibody formation in Aiolos null mice suggest its involvement in autoimmune disease (Wang et al., 1998; Sun et al., 2003). Finally, Aiolos is also involved in regulation of apoptosis via interactions with Ras and Bcl-x_L in the cytoplasm and also by exercise of transcriptional control over Bcl-2 gene expression (Romero et al., 1999; Rebollo et al., 2001).

Each of the Ikaros family members is characterized by the presence of up to four N-terminal DNA-binding zinc fingers and two C-terminal zinc fingers required for homo- and heterodimerization with other family members. Extensive alternative mRNA splicing of exons of Ikaros, Helios and Aiolos results in the expression of multiple isoforms of each protein that are differentially expressed in unique subsets of hematopoietic cells. The isoforms thus far described can be divided in two groups: those that possess at least three zinc fingers at the N-terminus and that bind DNA, and those with fewer than three N-terminal zinc fingers that are unable to bind DNA. Isoforms that cannot bind DNA but retain the capacity

to dimerize are considered to act in a dominant-negative fashion (Molnar and Georgopoulos, 1994; Kelley et al., 1998; Klug et al., 1998; Payne et al., 2001).

Several reports provide clues about how Ikaros family proteins regulate gene transcription. Aiolos and Ikaros proteins both recruit the Mi-2/NuRD and SIN3 histone deacetylase (HDAC)-containing repressor complexes (Koipally et al., 1999; Kim et al., 1999), and also the nucleosome-remodeling complex SWI/SNF to transcriptionally silenced regions of the genome (Kim et al., 1999; Koipally and Georgopoulos, 2002a; Georgopoulos, 2002). Additionally, Aiolos and Ikaros associate with CtBP-interacting protein (CtIP), which has been linked with HDAC-independent mechanisms of repression (Koipally and Georgopoulos, 2002b). To date, there have been no reports exploring the differential ability of isoforms to recruit these chromatin-modifying complexes.

Given the important role played in lymphoid development and apoptosis by the Aiolos gene in humans and mice, we need a better understanding of the various Aiolos isoforms present in the cell, and to address the physiological effects of the presence of functional domains.

In this article, we report our investigation into the type and functional significance of Aiolos isoforms. We have identified novel Aiolos transcripts in the peripheral blood of normal human subjects and in various cell lines derived from hematological malignancies. In order to study the functional differences between isoforms, we have cloned and expressed in mammalian cells five Aiolos isoforms with potentially different properties arising from their distinctive structures. We report the first direct comparison of the distribution, the association with components of the Mi-2/NuRD and SIN3 histone deacetylase complexes, the effects on the global levels of histone acetylation and direct binding to putative targets. Our results shed light on the relevance of the generation of complex patterns by multiple distinct functional Aiolos isoforms, some of which feature a partial loss of function. This implies the existence of combinatorial mechanisms that allow fine regulation by Aiolos.

Results

Identification of novel Aiolos isoforms

We first investigated the pattern of expression of different Aiolos isoforms in cell lines derived from B and T cell lymphoid malignancies. RT-PCR analysis of the Aiolos gene expression revealed nine novel Aiolos splicing variants (Fig. 1A) in addition to the seven isoforms previously reported (Liippo et al., 2001; Nakase et al., 2002) (Fig. 1B), although no characteristic isoform expression patterns were associated with any particular cell or sample type. Direct sequencing of the RT-PCR products enabled the characterization of these Aiolos variants, which we have systematically annotated after the exon that is missing. The isoforms are referred to here as Aio-Δ2 (lacking exon 2), Aio-Δ3 (lacking exon 3), Aio-Δ2,5 (lacking exons 2 and 5), Aio-Δ3,4 (lacking exons 3 and 4), Aio-Δ3,4,5 (lacking exons 3, 4 and 5), Aio-Δ3,4,5,6 (lacking exons 3, 4, 5 and 6), Aio-Δ4,5,6 (lacking exons 4, 5 and 6). The mRNA splice variants Aio-Δ2, Aio-Δ3 and Aio-Δ2,5 encode proteins with at least three N-terminal zinc-finger motifs within the DNA binding domain and, based on the properties of the highly homologous region of Ikaros, should retain the ability to bind DNA. The mRNAs Aio-Δ3,4, Aio-Δ3,4,5, Aio-Δ4,5,6 and Aio-Δ3,4,5,6 encode proteins lacking several zinc fingers within the DNA binding domain, which suggests they are unable to bind DNA and may act as dominant-negative isoforms (Molnar and Georgopoulos, 1994; Sun et al., 1996; Kelley et al., 1998; Klug et al., 1998; Payne et al., 2001; Sun et al., 1999).

Interestingly, the RT-PCR analysis also revealed two novel mRNAs derived from Aio-1 and Aio-Δ4 that contained a 126 bp insertion between exons 5 and 6. Direct sequencing of both variants showed that the insertion is derived from the Aiolos intron sequence between exons 5 and 6, and that it is flanked by splice donor and acceptor consensus sequences. We therefore consider this to be a novel exon, which we have called exon 5a. Accordingly, the two new variants containing exon 5a were named Aio-1-5a and Aio-Δ4-5a (lacking exon 4), respectively (Fig. 1B). The insertion of exon 5a introduces a stop codon into the Aiolos open reading frame and the encoded proteins have a distinct C-terminal region (Fig. 1B) that lacks the dimerization domain. All Aiolos isoforms previously described by other groups harbor the two C-terminal zinc finger motifs and may therefore form homo- and heterodimers (Liippo et al., 2001; Nakase et al., 2002). In addition, we used B cells from healthy subjects (15 samples) and from individuals diagnosed with systemic lupus erythematosus (10 samples) and rheumatoid arthritis (15 samples), two common autoimmune diseases (Fig. 1D). Aio-1 was in all cases the most abundant mRNA species in all the samples analyzed, although variable amounts of the different isoforms were observed. No obvious patterns in the expressed specific splice variant were found to be associated with any particular group of samples.

We also performed RT-PCR analysis of Aiolos gene expression in non-hematopoietic human cells such as the breast cancer cell line MCF 7, the hepatic cancer cell line HEPG2, the renal cancer cell line HEK, and a neuroblastoma-derived cell line SHSY-5Y. PCR products were transferred onto a nylon membrane and hybridized with a specific probe corresponding to a common region of all Aiolos isoforms in order to confirm the identity of the PCR bands (Fig. 1C). This analysis revealed that these cell lines express Aiolos isoforms in different proportions (Fig. 1C). COS-7 cells, by contrast, were found to be negative for Aiolos expression. No striking differences in the expressed specific splice variant were found to be associated with any particular cell type, tumorigenic potential or autoimmune disease.

Analysis of selected Aiolos isoforms

The presence of distinct recognized functional domains in the various Aiolos isoforms suggests that cells make use of combinations of different functional domains of the protein to modulate their function. In order to investigate the possible existence of distinct roles, we selected and cloned five Aiolos isoforms and generated their corresponding constructs for transfection in mammalian cells. The criteria for selection were based on choosing isoforms containing or lacking different well-defined functional domains. Aio-1, which can be considered the full-length isoform, contains all the exons and is the most abundant variant among the entire panel of cell types analyzed. Aio-1-5a, maintains an intact DNA binding domain but possesses a C-terminus that is different from all the other isoforms and, therefore, lacks the two C-terminal zinc fingers involved in homo- and heterodimerization. In Aio-Δ5,

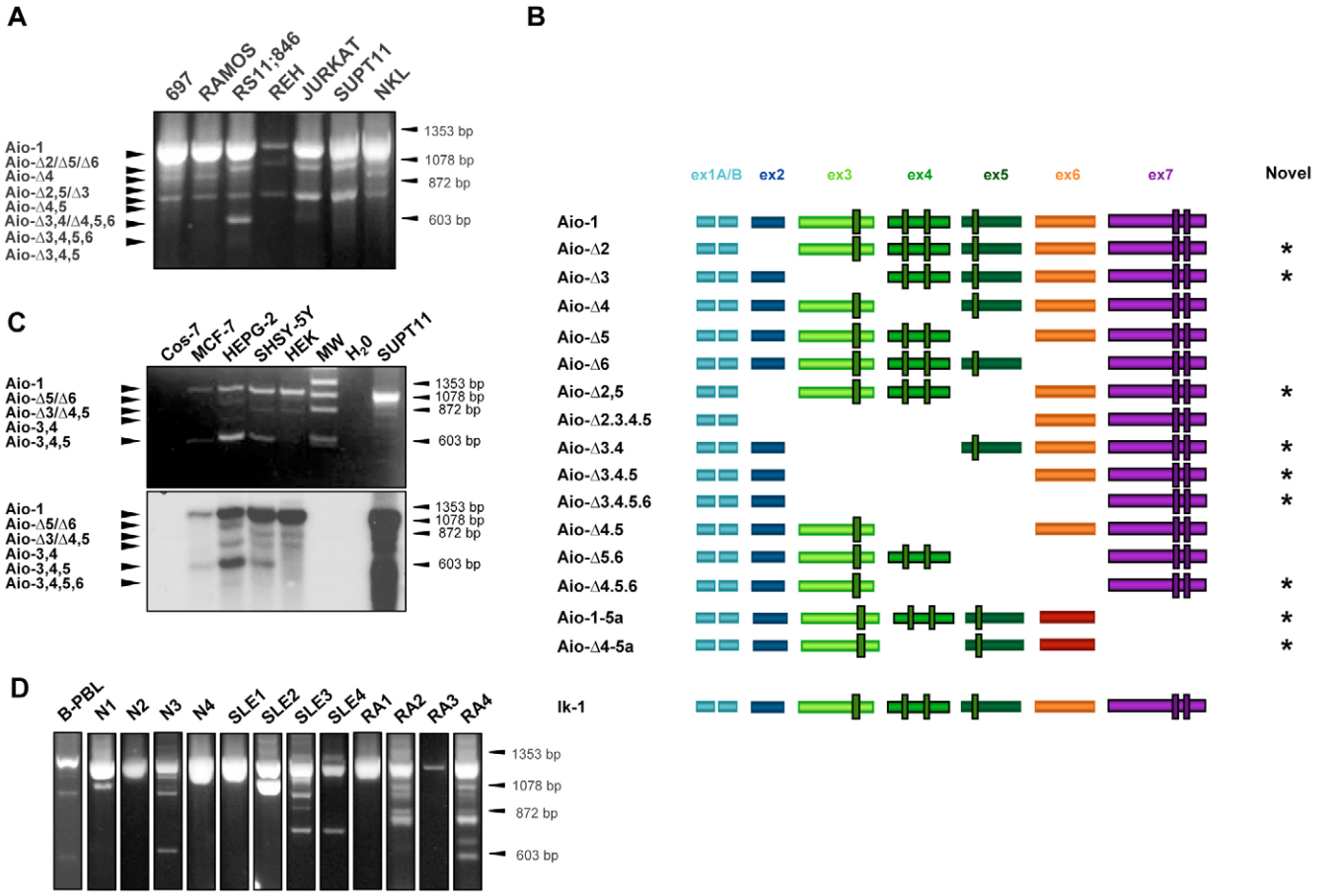

Fig. 1. The Aiolos gene codes multiple isoforms. (A) A representative RT-PCR with primers corresponding to exon 1 and 7 in hematopoietic cell lines derived from human B leukemic (697, RAMOS, RS11;846, REH) and T leukemic (JURKAT, SUPT11) cells and the NKL cell line, derived from natural killer (NK) cells. (B) Schematic representation of Aiolos isoforms. Green boxes in exons 3-5 indicate the four N-terminal zinc finger motifs involved in DNA binding and the two violet boxes in exon 7 indicate the C-terminal motifs required for dimer formation. The two Aiolos isoforms (at the bottom) contain an alternative exon, which we have named exon 5a (see Results). Aiolos isoforms have been named according to the exons missing from the full-length isoform. Ikaros full-length isoform Ik-1 is also shown at the bottom. Nine novel Aiolos isoforms are indicated on the right by asterisks. (C) RT-PCR analysis of non-hematopoietic human cell lines (monkey SV40-transformed fibroblast cell line COS-7, breast cell line MCF 7, liver cell line HEPG2, a neuroblastoma-derived cell line SHSY-5Y and kidney cell line HEK) also show the presence of multiple Aiolos isoforms. Molecular weight (MW) markers are included. PCR products were transferred onto a nylon membrane and hybridized with a specific C-terminal Aiolos probe in order to confirm the identity of the PCR bands (bottom panel). (D) Representative RT-PCR analysis of B cells including B-cell-derived lymphoblastoid cells (B-PBL), and samples from healthy subjects (N1-N4) and individuals with systemic lupus erythematosus (SLE1-SLE4) and rheumatoid arthritis (RA1-RA4).

one of the zinc fingers at the N-terminus is missing, but the protein retains the ability to associate with DNA. The isoforms Aio-Δ3,4,5 and Aio-Δ3,4,5,6 have lost the DNA binding domain but retain the dimerization domain (Fig. 2A).

The cDNAs of Aiolos isoforms Aio-1, Aio-1-5a, Aio-Δ5, Aio-Δ3,4,5 and Aio-Δ3,4,5,6 were subcloned into an expression vector containing a sequence encoding the FLAG epitope. For transient transfection experiments, we selected COS-7 cells, which do not express either the Aiolos or the Ikaros genes (see Fig. 1C) (Cobb et al., 2000; Koipally and Georgopoulos, 2002a), providing a system in which the individual effects of Aiolos isoforms can be investigated without interference with endogenous Aiolos or Ikaros (for instance, through dimerization). In addition, COS-7 cells constitute an excellent system for this type of study where transfection is achieved at a very high efficiency and cells are convenient for immunocytochemistry experiments. After transfection, the presence of stable recombinant Aiolos proteins in COS-7 cell extracts was verified by western blot with both a mouse monoclonal anti-FLAG antibody and a polyclonal anti-Aiolos antiserum of transfected COS-7 cell extracts. As shown in Fig. 2B, all the constructs were properly transcribed and produced stable proteins in COS-7 cells.

Isoform-specific cell distribution of the Aiolos variants

Before doing a functional study, we investigated the individual localization of the five Aiolos isoforms. The distribution of the different Aiolos isoforms, transiently transfected in COS-7 cells, was determined by immunofluorescence and confocal microscopy using a mouse monoclonal anti-FLAG antibody.

These immunocytochemistry experiments revealed an isoform-specific cell distribution in the Aiolos isoforms. Aio-

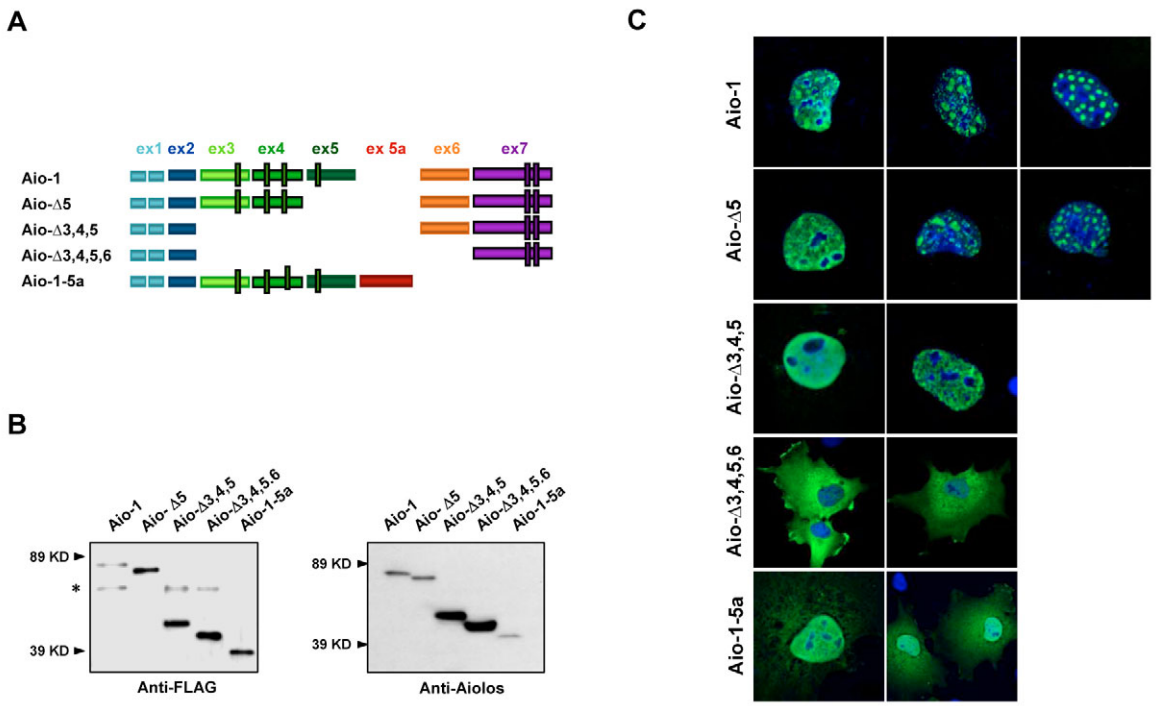

Fig. 2. Transfection of Aiolos isoforms in mammalian cells. (A) Schematic representation of the five selected isoforms. (B) Western blot of COS-7 cells extracts transfected with the five Aiolos isoforms and developed with the mouse monoclonal anti-FLAG antibody (left) and a polyclonal anti-Aiolos antiserum (right). (C) Subcellular localization of Aiolos isoforms. Confocal images of COS-7 cells transfected with different Aiolos isoforms and labeled with antibody to Aiolos (green). Nuclear DNA was counterstained with DAPI (blue). Images of different subpopulations are included (indicated in Results).

1, the full-length isoform of Aiolos, and Aio-Δ5, the isoform lacking just one zinc finger, are both present in nuclei, but are excluded from the nucleoli. These two isoforms exhibit a similar pattern of distribution in COS-7 cells and two populations can be distinguished. 70-80% of the cells have a diffuse nuclear distribution, tending to concentrate in the perinuclear heterochromatin. The remaining 20-30% of the cells have a more restricted distribution with speckles of variable diameter (1-6 μm) (Fig. 2C). These data are consistent with previous reports of a cell-cycle-dependent distribution of Ikaros (e.g. Brown et al., 1997). Brown and coworkers also observed a striking coincidence between Ikaros and DAPI staining. S-phase cells appeared to express similar levels of Ikaros to G1-phase cells but distributed as a fine haze, whereas cells in G1 and G2 phases exhibited a pattern of intense foci (Brown et al., 1997; Dovat et al., 2002).

By contrast, the Aio-Δ3,4,5,6 isoform, which lacks the DNA-binding domain, was predominantly localized in the cytoplasm (Fig. 2C) and cytoplasmic membrane, similar to the distribution described for the Ikaros dominant-negative isoforms (Morgan et al., 1997; Romero et al., 1999). The fact that the Aio-Δ3,4,5,6 variant maintains the dimerization domain and may be able to bind other nuclear proteins could account for why a small fraction localizes to the nucleus. Aio-Δ3,4,5, which also lacks the ability to bind DNA and differs from the previous isoform only in the presence of exon 6, was found throughout the nucleus, except in the nucleolus (Fig. 2C). This suggests that, besides the contribution of the DNA-binding domain to target Aiolos to the DNA within the nucleus, exon 6 may account for the import of this protein into the nucleus. This notion is supported by the findings of studies of isoform Aio-1-5a (see Fig. 2C), which possesses an intact DNA binding domain but a distinct C-terminal region that contains exon 5a, but not exons 6 and 7, and shows both a nuclear and cytoplasmic punctuate distribution.

Ikaros and Aiolos distribution are modulated through heterodimerization in an isoform-dependent fashion

All the transfected Aiolos isoforms except isoform Aio-1-5a have a dimerization domain at their C-terminus. Previous studies of Ikaros and Aiolos have shown that this domain enables these proteins to form both homo- and heterodimers with other proteins of the family (Morgan et al., 1997; Georgopoulos et al., 1997). It has also been shown that Helios forms multimeric complexes with Ikaros in hematopoietic cells (Hahm et al., 1998). In order to investigate how the formation of heterodimers influences subcellular localization, we cotransfected COS-7 cells with Ikaros-1 (Ik-1) and the Aiolos isoforms. We then performed immunocytochemistry and confocal microscopy with the anti-FLAG and anti-Ikaros antibodies.

We observed that Ikaros-1 has an identical pattern of localization to that of Aio-1 isoform. In these experiments, we found a 90-98% colocalization between Ik-1 and all Aiolos isoforms, except Aio-1-5a. As shown in Fig. 3, isoforms Aio-1 and Aio-Δ5 colocalize with Ik-1 isoform in the cell nucleus and their distribution is identical to that of Aiolos in single transfection experiments, where 80% of the cells exhibit a diffuse nuclear pattern and 20% have a speckled pattern that is restricted to heterochromatic regions. Aio-Δ3,4,5 also

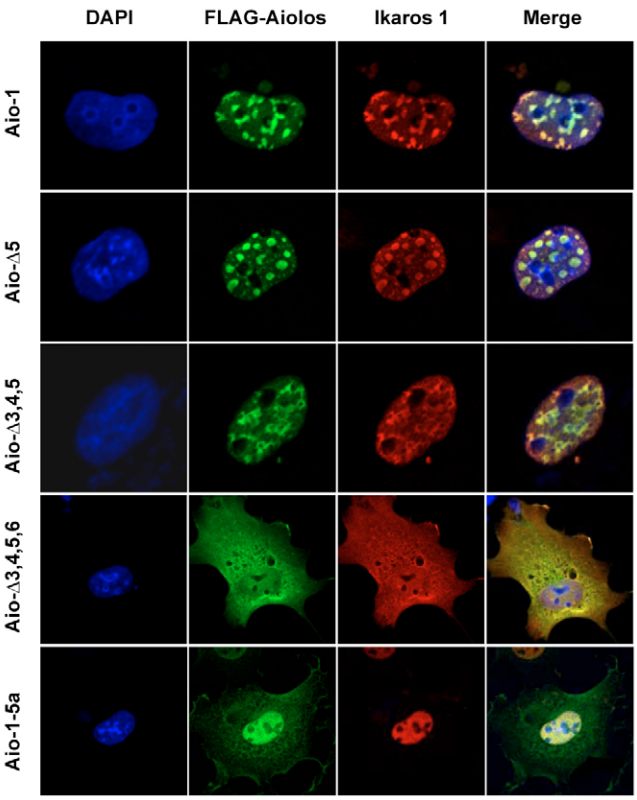

Fig. 3. Subcellular localization in COS-7 cells of Aiolos isoforms cotransfected with Ikaros-1. Aiolos isoforms were labeled with Cy2 (green) and Ikaros-1 was labeled with Cy3 (red). Nuclei were counterstained with DAPI (blue).

colocalizes with the Ik-1 isoform. However, although the same type of distribution as that of the single transfection of Aio-Δ3,4,5 was seen in the majority of the cells, in approximately 10% of the cells it had a more localized distribution pattern. Interestingly, cotransfection of Aio-Δ3,4,5,6 with Ik-1 result in mutual influence in the localization patterns. Ik-1, which in the absence of Aiolos is located exclusively in the nucleus, when expressed in the presence of Aio-Δ3,4,5,6, is also found in the cytosol, where these two proteins colocalize to an extent of more than 90% (Fig. 3). Conversely, the presence of Ik-1, and subsequent heterodimerization with Aio-Δ3,4,5,6, moves this isoform into the nucleus (Fig. 3). We can hypothesize that isoforms lacking DNA-binding domains play a role in sequestering or quenching other isoforms through heterodimerization. This ability would confer a dominant-negative character on this type of Aiolos isoform, as already suggested in early work by Molnar and Georgopoulos (Molnar and Georgopoulos, 1994).

Finally, although both Ik-1 and Aio-1-5a localize in the nucleus, the slight overlap between them can be easily explained by the absence of the dimerization domain in the Aio-1-5a isoform.

Differential isoform-specific association with histone deacetylase-containing complexes

Previous data indicate that Aiolos interacts with Mi-2/NuRD and SIN3 histone deacetylase complexes (Koipally et al., 1999). There is also an association between Aiolos and SWI/SNF complexes (Kim et al., 1999). However, all these studies were carried out using the Aio-1 isoform. Here we have examined the possibility that Aiolos isoforms vary in their degree of association with histone deacetylase-containing complexes. We performed immunoprecipitation of total extracts from transfected COS-7 cells with anti-FLAG antibodies, followed by western blot with several antibodies against HDAC1, a histone deacetylase common to the SIN3 and Mi-2/NuRD complexes. In addition, to determine the specific association with the Mi-2/NuRD and SIN3 complexes, we used antibodies against SIN3A, and MTA1, MTA2 and MTA3, which have been shown to define three different subfractions of the Mi-2/NuRD complex (Bowen et al., 2004; Fujita et al., 2003; Fujita et al., 2004).

Analysis of immunoprecipitated fractions showed that comparable amounts of Aiolos isoforms coimmunoprecipitated significantly different amounts of the above factors (Fig. 4A). We observed that Aio-1 has the strongest affinity for both HDAC1 and Mi-2/NuRD subunit MTA2 relative to the other isoforms (Fig. 4A). No interactions with MTA1 and MTA3 were observed. Therefore, our data indicate that Aiolos specifically recruits the MTA2 subfraction of the Mi-2/NuRD complex. Only Aio-1 also appeared to interact with SIN3A.

We then studied the colocalization of Aiolos isoforms with HDAC1, SIN3 and MTA2 in COS-7 cells by immunocytochemistry and confocal microscopy. We observed that in control untransfected COS-7 cells these three factors have a homogeneous localization, similar to the pattern described by others (Yang et al., 2002; Humphrey et al., 2001) (Fig. 4B).

We found that that is more than 90% colocalization of the Aio-1 isoform with HDAC1 and MTA2 (Fig. 4C). By contrast, transfection with Aio-1 did not change the diffuse pattern of SIN3A. This is in agreement with the results obtained from the immunoprecipitation study (Fig. 4A).

In Aio-Δ5- and Aio-Δ3,4,5-transfected cells, similar patterns of distribution of Aiolos and HDAC1 and MTA2 were observed, although the levels of colocalization were significantly lower than those in Aio-1. Colocalization between Aio-Δ3,4,5,6 and Aio-1-5a with HDAC1 and MTA2 is very slight (Fig. 4C), as expected from their structures.

Functional effects of Aiolos isoforms on histone modifications

Once we had confirmed the association of Aiolos isoforms with histone deacetylase complexes, and the varying degrees of colocalization, we investigated the direct effects of Aiolos isoforms on the acetylation patterns of histones. To this end, we used two methods to analyze the acetylation levels of histones H3 and H4 in COS-7 cells transfected with the Aiolos isoforms: western blot with specific antibodies against different histone acetylation sites, and capillary electrophoresis of HPLC-fractionated histone fractions (see Materials and Methods). Interestingly, we found that transfection with Aio-1, Aio-Δ5 and Aio-1-5a significantly affected the global acetylation levels of histones H3 and H4 (Fig. 5A), whereas no differences were observed for Aio-Δ3,4,5 and Aio-Δ3,4,5,6 when compared with mock-transfected cells. Changes were observed not only with antibodies against hyperacetylated

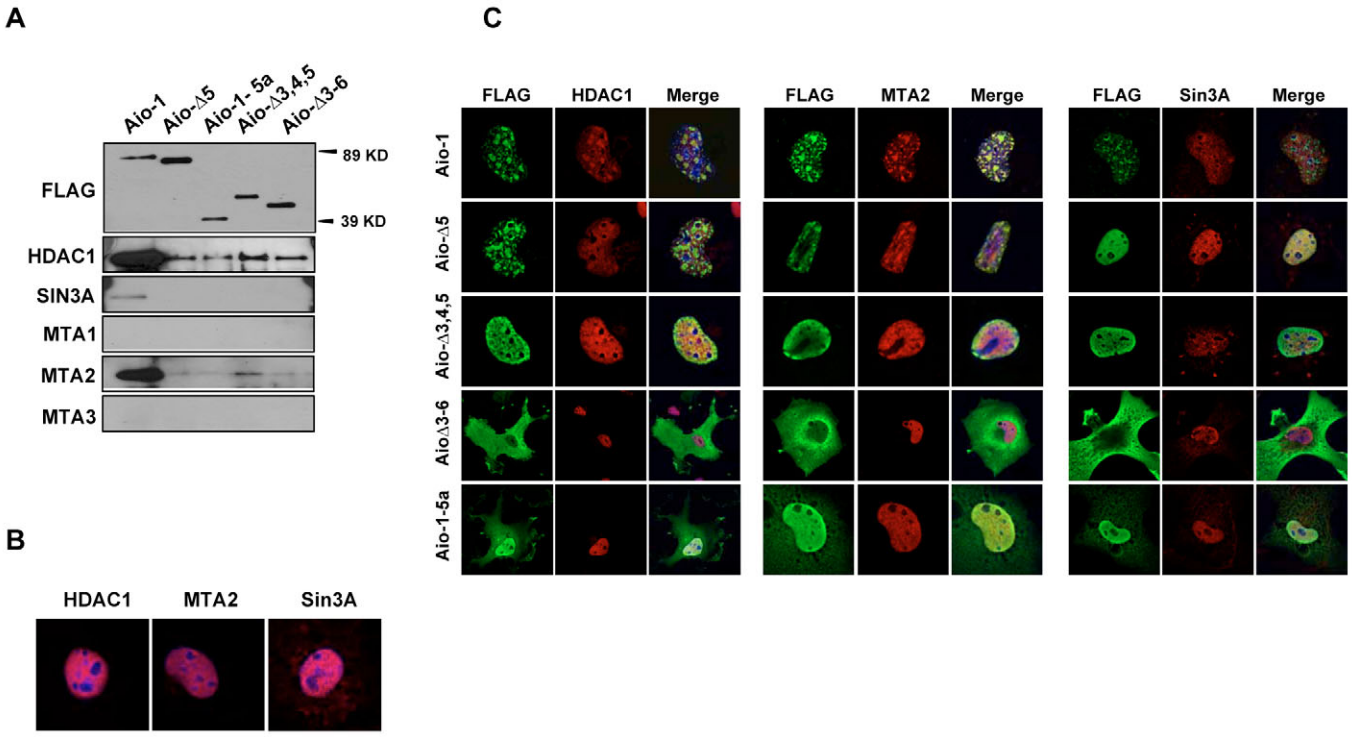

Fig. 4. Association of Aiolos isoforms with histone deacetylase. (A) In vivo interaction between Aiolos isoforms and components of the Mi-2/NurD and SIN3 histone deacetylase complexes. Immunoprecipitation of Aiolos was accomplished using an anti-FLAG antibody and eluates were tested by immunoblot analysis with anti-FLAG, anti-HDAC1, anti-SIN3A and three antibodies that each distinguish a subfraction of the Mi-2/NuRD complex, namely anti-MTA1, anti-MTA2 and anti-MTA3. Input COS-7 cell extracts were tested for all antibodies (not shown). (B) Confocal images of untransfected COS-7 cells showing distribution of HDAC1, SIN3A and MTA2. (C) Confocal images of COS-7 cells transfected with different Aiolos isoforms. Aiolos isoforms were stained with an anti-FLAG and a secondary anti-mouse labeled with Cy2 (green). HDAC1, MTA2 and SIN3A were labeled with Cy3 (red). Nuclei were counterstained with DAPI (blue).

histones H3 and H4, but also with antibodies specific for certain lysine amino acid residues, such as K8 and K16 of histone H4 and K9 of histone H3.

We also used high-performance capillary electrophoresis (HPCE) to quantify global acetylation levels of histone H4 in the COS-7 cells before and after transfection with the five Aiolos isoforms. Around 40% of total histone H4 was found to be constitutively acetylated in COS-7 cells (35.9±1.3) or mock-tranfected COS-7 cells (36.2±1.0), which is similar to the basal acetylation levels previously found in immortalized human cell lines (Fraga et al., 2005). Transfection with the construct encoding Aio-1 resulted in a decrease in the levels of histone H4 acetylation (percentage relative acetyl H4 of 29.4±0.9) which was found to be statistically significant (*t*-test with respect to mock-transfected control, P=0.0009; Fig. 5C), primarily as a result of the loss of monoacetylated histone H4. Expression of the isoforms Aio-1-5a and Aio-Δ5, which maintain the ability to bind DNA, also caused a decrease in global H4 acetylation (percentage relative global acetyl H4 of 30.5±1.1 and 32.7±0.8, respectively) statistically significant (P=0.0027 and P=0.0091 as calculated by *t*-test comparison of means) although overexpression of isoforms not expected to bind DNA (Aio-Δ3,4,5 and Aio-Δ3,4,5,6) did not result in any change in the global histone H4 acetylation status (36.8±1.2 and 37.2±1.4; Fig. 5C) as confirmed by *t*-tests (P=0.543 and 0.371, respectively).

Aiolos isoforms differentially associate with the promoter of target genes

As a member of a family of transcriptional regulators, we would expect transfection with Aiolos to lead to a change in the expression pattern of a number of genes. We have used microarrays to analyze gene expression of COS-7 cells transfected with Aiolos isoform Aio-1 (data not shown). Introduction of Aiolos resulted in both overexpression and downregulation of a number of genes (R.C., M.A., M.E., R.G.-S. and E.B., unpublished). Among the genes that were validated by quantitative real-time RT-PCR, several key genes are of note. It is remarkable that transfection of COS-7 cells with Aio-1 resulted in a consistent 20% downregulation of SIRT1 (silent mating type information regulation 2, SIR2, homolog), a class III NAD-dependent histone deacetylase that is thought to participate in the formation of facultative heterochromatin (Vaquero et al., 2004).

Changes in the expression levels of a gene may have two possible causes: direct association of Aiolos with the regulatory region of the target gene, or indirect regulation through changes in the expression of another transcriptional factor, targeted by Aiolos, and consequent deregulation of a number of downstream targets. Thus, we decided to investigate the association of Aiolos Aio-1 with the promoter of a number of dysregulated genes, including the SIRT1 promoter, and to compare the association of the remaining Aiolos isoforms, by

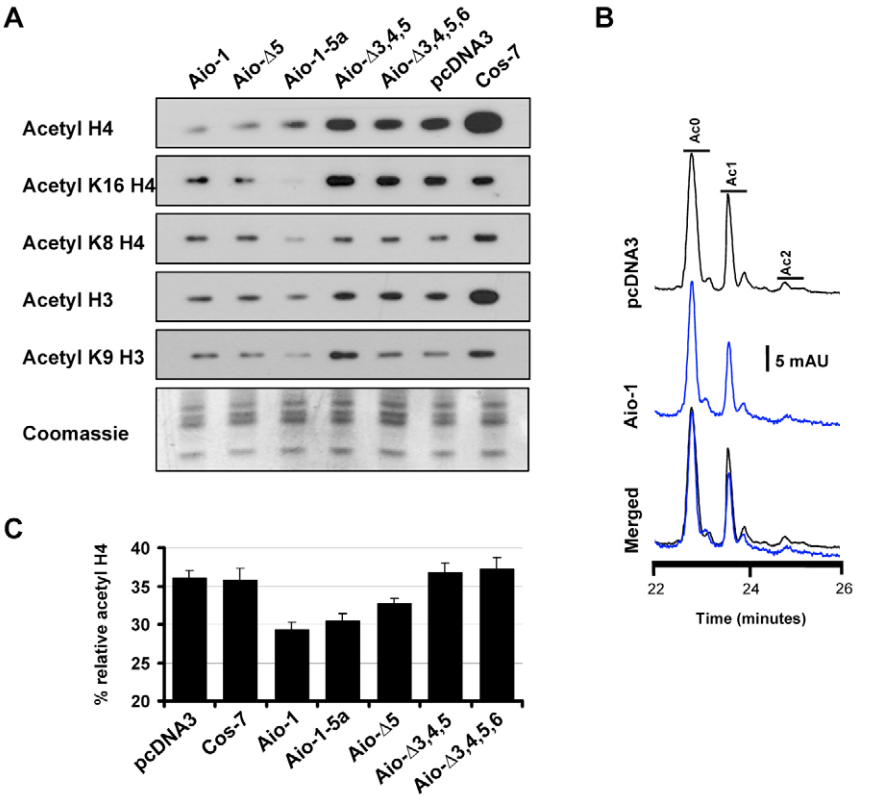

Fig. 5. Effects on global histone acetylation patterns of COS-7 cells transfected with Aiolos isoforms. (A) Western blot analysis of histone modifications of cell extracts. Analysis with antibodies against acetyl-H4, acetyl K16 and K8 of H4, acetyl-H3 and acetyl K9 of histone H3. A Coomassie Blue staining is also shown as a loading control. (B) Analysis of histone H4 acetylation by high performance capillary electrophoresis (HPCE). An example of HPCE separation of acetylated species of histone H4 from pcDNA3 and Aiolos-transfected COS-7 cells. The non-acetylated (Ac0), monoacetylated (Ac1) and diacetylated (Ac2) forms of histone H4 are indicated. (C) A quantification of the HPCE analysis showing the acetylation of histone H4 corresponding to COS-7 cells transfected with all Aiolos isoforms.

performing a chromatin immunoprecipitation (ChIP) analysis (Orlando, 2000). This assay can determine whether a particular transcriptional factor (Aiolos, in this case) is bound to a specific promoter in its natural chromatin state (in this case, the promoter of downregulated genes obtained from the microarray analysis). Immunoprecipitated DNA with anti-FLAG antibodies and Anti-Aiolos antiserum was then analyzed by PCR with specific primers for the promoters. Before the primers were designed we studied a fragment containing the DNA binding site for Aiolos (TGGGAA). We found Aio-1 to be specifically associated with the promoter of SIRT1 (Fig. 6A), which implies a potential role for Aiolos in the regulation of SIRT1 expression. ChIP analysis with the remaining isoforms showed that Aio-Δ5 and Aio-1-5a were both also associated with the SIRT-1 promoter (Fig. 6A). As expected, Aio-Δ3,4,5 and Aio-Δ3,4,5,6, which lack the DNA-binding motifs, do not associate with the SIRT1 promoter.

Aiolos isoforms in B cells

As introduced above, Aiolos has a key role in hematopoietic differentiation, in particular in B cells. Although the Aiolos isoforms analyzed in the present study were identified and isolated in B cells, all the above experiments were performed in COS-7, a fibroblast cell line. As described, this system is ideal for several reasons. However, the results obtained might depend on that particular cell context and it is important to assess whether these results are relevant to the B-cell system. In order to investigate some of the properties described above in a cell type more relevant to the hematopoietic system we decided to use two cell types: RAJI cells, a Burkitt's lymphoma cell line derived from B lymphocytes, and B-cell-derived lymphoblastoid cells, an Epstein-Barr virus (EBV)-transformed lymphoblastoid cell line. These two cell types express Aiolos (data not shown) and can be transfected with FLAG-tagged Aiolos expression vectors to investigate the properties of Aiolos isoforms.

Interestingly, immunocytochemistry experiments in transiently transfected RAJI and B-PBL cells revealed an isoform-specific distribution very similar to that obtained in COS-7 cells (Fig. 7A). Similar to experiments with COS-7 cells, in RAJI and B-PBL cells the Aio-1 and Aio-Δ5 isoforms are found in the nucleus, with a diffuse distribution in the majority of cells and a more restricted speckled distribution in a smaller fraction of cells. Interestingly, the Aio-Δ3,4,5,6 isoform, which lacks the DNA-binding domain and is predominantly localized in the cytoplasm and membrane in COS-7 cells (Fig. 2C), is present as two populations in RAJI and B-PBL cells, the predominant one in nuclei, cytosol and membranes, and a second one where it is excluded from the nuclei (Fig. 7A,B). This can easily be explained if we take into account that endogenous Aiolos (or Ikaros), expressed in RAJI and B-PBL cells, can dimerize with isoform Aio-Δ3,4,5,6. These results would be in agreement with the data shown in Fig. 3, where co-transfection with Ik-1 modulates isoform Aio-Δ3,4,5,6 localization.

When studying colocalization of Aiolos isoforms with HDAC1 in RAJI and B-PBL cells, we observed a high degree of colocalization between the Aiolos fraction in the nucleus and HDAC1 (Fig. 7B). We found that the cytosolic fraction of Aio-Δ3,4,5,6 and Aio-1-5a do not colocalize with HDAC1, in agreement with data obtained in COS-7 cells.

Discussion

It is well established that many human genes are alternatively

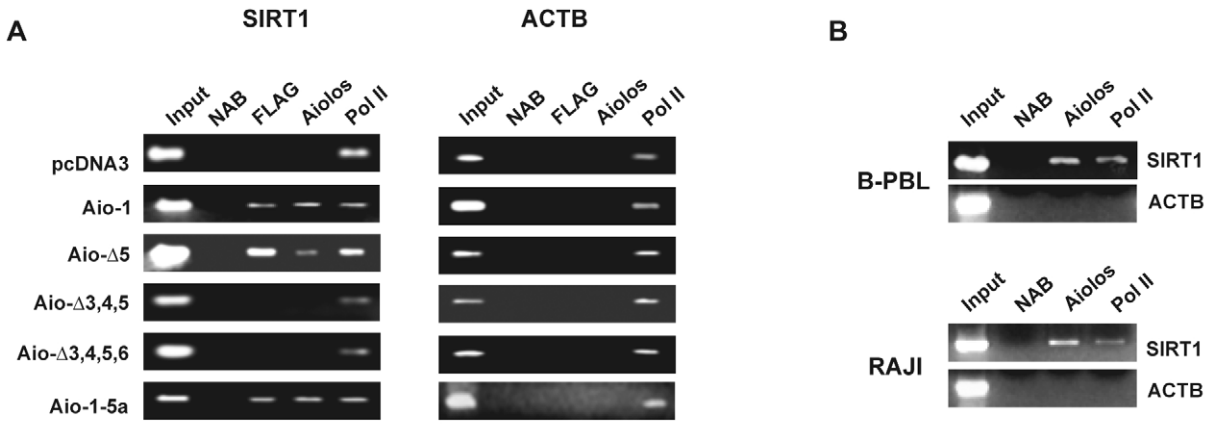

Fig. 6. Analysis of the interaction of Aiolos isoforms with the promoter of SIRT1. (A) ChIP assays were performed with anti-FLAG, anti-Aiolos and anti-RNA pol II antibodies in COS-7 cells transfected with all the Aiolos isoforms studied in this work. Negative controls (No antibody, NAB) are also shown. Input and bound fractions are shown. In addition to the SIRT1 promoter, actin B gene promoter was used as a negative control. (B) Association of Aiolos to the SIRT1 promoter in B cells. ChIP assays in untransfected RAJI and B-PBL cells. Anti-Aiolos and anti-RNA pol II antibodies were used. Actin B was used as a negative control.

spliced and that this multiplicity is an effective way to increase the diversity of proteins derived from a single gene. These proteins generated by alternative splicing can differ in subtle or dramatic ways by deleting regions involved in interactions with partners or localization (Lareau et al., 2004). All the Ikaros family members, master regulators of hematopoietic differentiation, exhibit multiple isoforms, including Aiolos, the object of our study. The prevalence of alternatively spliced Ikaros family proteins raises intriguing questions regarding their function and the selective advantage that they may confer. At any rate, the alternative splicing affecting defined functional domains appears to be an effective way of regulating their biological behavior. Furthermore, the ability of Ikaros family members to homo- and heterodimerize adds an extra layer of complexity, since modulation involves the dimers and multimers of multiple isoforms of different Ikaros family members.

We have examined the features that make different isoforms unique: how the presence of different combinations of functional domains is reflected in a range of biological properties including cell localization, association with Ikaros and various components of histone deacetylase complexes; effects on histone acetylation; and association with putative target genes. These results are summarized in Table 1. They indicate that the full-length isoform of Aiolos, Aio-1, possesses all the major functions, as would be anticipated from an appreciation of its well-defined functional domains, consistent with previous findings (Koipally et al., 1999). Moreover, we have confirmed that the remaining isoforms have lost function associated with the missing functional domain. We propose that the isoforms that lack certain domains and show a partial loss of function could probably have an important role in modulating the activity of full-length isoforms by interacting with them. This is observed in experiments in which Aiolos isoforms have been co-transfected with Ikaros. For example, the co-transfection of Aio-Δ3,4,5,6 and full-length Ikaros isoform (Ik-1) results in a change of cellular distribution of both proteins, probably as a result of heterodimerization.

Regarding the cellular distribution of the Aio-Δ3,4,5,6 isoform, we have observed an interesting difference with respect to that of Aio-Δ3,4,5, which only differs in exon 6. This finding has prompted us to propose the existence of a nuclear localization signal in exon 6. Although no consensus NLS has been described, most of the experimentally characterized NLSs are monopartite and bipartite motifs, both of which are characterized by clusters rich in basic amino acid residues (Cokol et al., 2000). Exon 6 is particularly rich in basic amino acid residues and has indeed a much more basic pKa than that of the full-length protein (11.18 versus 6.15). Therefore, we suggest that this high concentration of basic residues in exon 6 may indicate an NLS. This is supported by the findings of studies of isoform Aio-1-5a (see Fig. 2C), which possesses an intact DNA binding domain but a distinct C-terminal region that contains exon 5a, but not exons 6 and 7, and shows both a nuclear and cytoplasmic punctuate distribution. Schmitt et al. (Schmitt et al., 2002) have suggested that Tyr 286, corresponding to exon 7 from the genomic sequence, is involved in nuclear localization, as Tyr to Thr abrogates translocation to the nucleus, whereas other mutants do not exhibit such an effect. Our results indicate that nuclear localization depends not only on Tyr 286 in exon 6 but also on the presence of exon 6.

It has been suggested that alternative splicing often creates novel isoforms by the insertion of new, functional protein sequences that probably originate from non-coding sequences of introns. This appears to be the case with Aio-1-5a and Aio-Δ4-5a, two novel isoforms described in this report that lack the dimerization domain at the C-terminus. We have analyzed and compared the functionality of Aio-1-5a in our study. This isoform exhibits nuclear and cytoplasmic localization and interacts weakly with Mi-2/NuRD and SIN3 histone deacetylase complexes. Immunofluorescence analyses have shown a small overlap with Ikaros, reinforcing the notion that absence of the C-terminal dimerization motif prevents interaction with other Ikaros family members. However, we have observed that transfection with Aio-1-5a affects global acetylation status, and binding to SIRT1 has been demonstrated. These findings suggest that the activity of these

isoforms is independent of the interaction with other Ikaros family members.

An expression microarray study performed with Aio-1 revealed that SIRT1, a NAD^+-dependent histone deacetylase is downregulated in cells transfected with Aio-1. This finding is particularly interesting considering that SIRT1 has been associated with the formation of facultative heterochromatin (Vaquero et al., 2004) and Aiolos is localized in pericentromeric heterochromatin during some phases of the cell cycle. But we have observed that not only Aio-1 but also Aio-Δ5 and Aio-1-5a (which have different properties from the full-length isoform, as described in this work; see Fig. 6) associate with the SIRT1 promoter. Remarkably, the generality of our conclusions with COS-7 cells is highlighted by the fact that Aiolos also binds the promoter of SIRT1 in both RAJI and B-PBL cells (Fig. 6B). We may speculate that the expression of different combinations of Aiolos isoforms would modulate the effects on the expression levels of SIRT1. In addition, isoforms lacking more than three zinc fingers of the DNA-binding domain, such as Aio-Δ3,4,5,6, might quench a fraction of Aio-1 and therefore reduce the fraction of Aio-1 interacting with the SIRT1 promoter.

In this study we have analyzed the expression patterns of Aiolos isoforms in cells derived from different lymphoid malignancies and samples from individuals diagnosed with rheumatoid arthritis and systemic lupus erythematosus, in which lymphocyte function is misregulated. These analyses have led us to identify a number of novel isoforms, although we found no specific patterns of isoform expression. The absence of such patterns does not rule out the possible involvement or contribution of these isoforms to the disease. In fact, Aiolos-deficient mice (Wang et al., 1998; Sun et al., 2003) develop the symptoms of human systemic lupus erythematosus.

The analysis of Aiolos isoforms in different cell types, by transfection experiments, has allowed their potential individual contribution to Aiolos function to be predicted. Our findings attest to the complexity of regulation by the combinations of splice variants. It is likely that subtle differences in the levels of expression account for significant alterations in Aiolos function and thereby the misregulation of key genes in lymphocyte behavior.

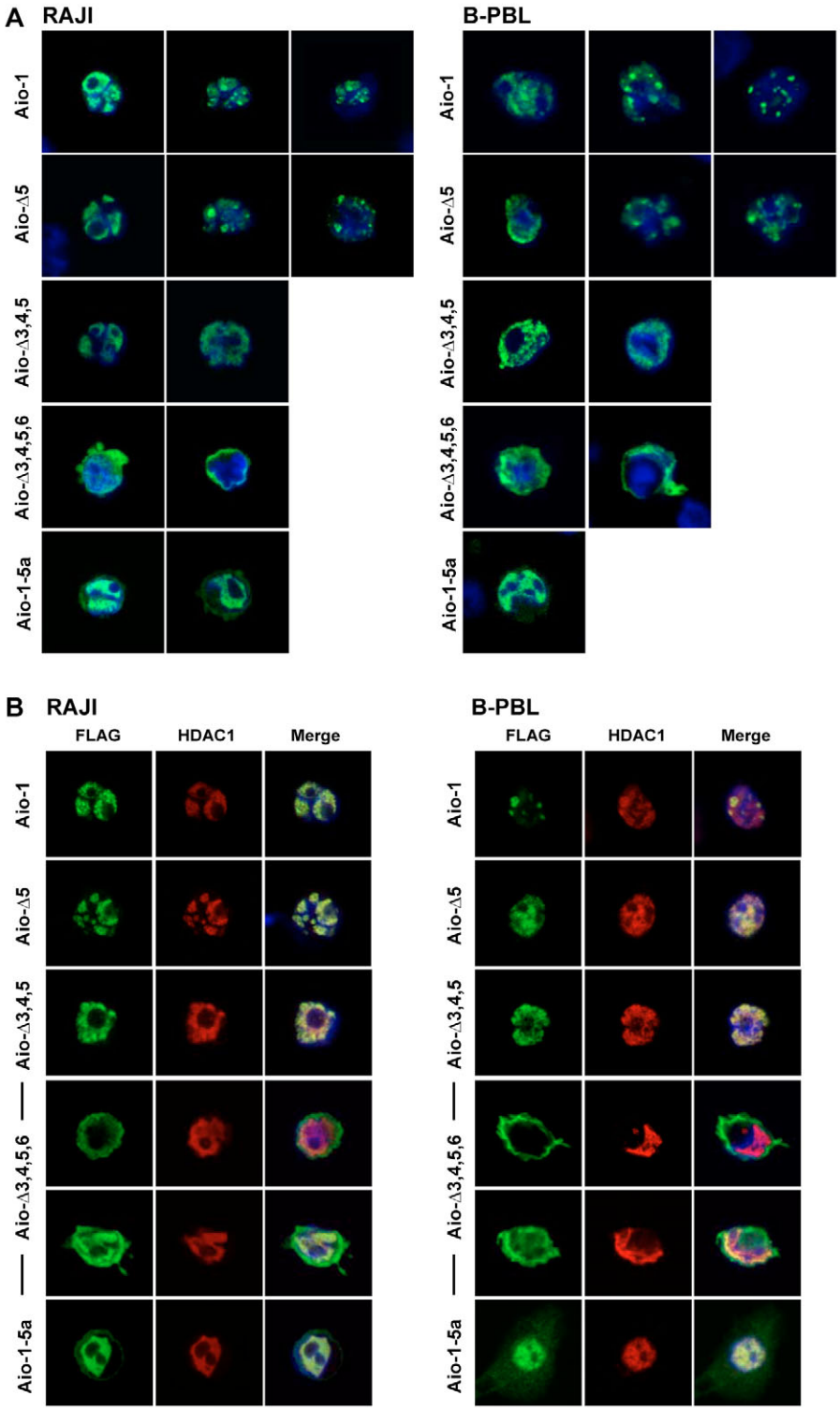

Fig. 7. Transfection of Aiolos isoforms in B cells. (A) Subcellular localization of Aiolos isoforms. Confocal images of RAJI and B-PBL cells transfected with different Aiolos isoforms and labeled with Aiolos antibody (green). Nuclear DNA was counterstained with DAPI (blue). Images of different subpopulations are included (indicated in Results). (B) Association of Aiolos isoforms with histone deacetylase. Confocal images of RAJI and B-PBL cells transfected with different Aiolos isoforms. Aiolos isoforms were stained with anti-FLAG and a secondary anti-mouse antibody, labeled with Cy2 (green). HDAC1 was labeled with Cy3 (red). Nuclei were counterstained with DAPI (blue).

Table 1. Summary of the properties of the five Aiolos isoforms studied

	Aio-1	Aio-Δ5	Aio-Δ3,4,5	Aio-Δ3,4,5,6	Aio-1.5a
Nuclear localization	*	*	*		*
Cytosolic localization				*	*
Heterodimerization with Ikaros	*	*	*	*	
HDAC1 interaction	++++	+	++	+	+
Sin3 interaction	+				
MTA2 interaction	++++	+	++	+	+
Effects of histone acetylation	*	*			*
Interaction with SIRT1 promoter	*	*			*

*, property is present/exhibited by the corresponding isoform; +, property is present at the level indicated (+, ++, +++).

Materials and Methods

Materials

The following cell lines were used: hematopoietic cell lines derived from human B leukemic (697, RAMOS, RS11;846, REH) and T leukemic (JURKAT, SUPT11, MOLT4, MOLT16) cells, myeloid cell lines (HL-60, MV4;11), lymphoma cell lines (NAMALWA, RAJI), the NKL cell line, derived from natural killer (NK) cells and a B-cell-derived EBV-transformed lymphoblastoid cell line (B-PBL). Also, non-hematopoietic cell lines (monkey SV40 transformed fibroblast cell line COS-7, the breast cell line MCF 7, liver cell line HEPG2, a neuroblastoma-derived cell line SHSY-5Y and kidney cell line HEK) were analyzed. Cell lines were maintained in RPMI1640 (Bio-Whittaker) or DMEM (Gibco, Invitrogen) supplemented with 10% fetal calf serum (FCS; HyClone) and 1% penicillin-streptomycin (Bio-Whittaker). In addition, mononuclear cells were obtained from peripheral blood of rheumatoid arthritis patients, systemic lupus erythematosus patients and healthy donors who gave informed consent to the study. Peripheral lymphocytes were purified by gradient centrifugation using Ficoll (Histopaque®-1077, Sigma).

Cell transfections

Transient transfection of COS-7 cells was performed with Lipofectamine 2000 reagent (Invitrogen) following the instructions of the manufacturer. In the case of RAJI and B-PBL cells, transient transfection was performed by electroporating 10^7 cells in 0.8 ml PBS with 40 μg of the vector at 250 V and 975 μF. After electroporation, cells were washed with PBS and seeded at 10^6 cells/ml in fresh medium containing 20% FBS.

RNA extraction and reverse transcription-polymerase chain reaction (RT-PCR) analysis

Total RNA was isolated from human B- and T-leukemic cell lines and non-haematopoietic cell lines as well as from mononuclear cells obtained from peripheral blood of both patients and healthy volunteers, using Trizol (Invitrogen). cDNA synthesis was performed with the IMPROM-II kit (Promega) from total RNA (2 μg). RT-PCR was performed with primers designed in exon 1 (Aiol-ex1F, 5′-ATGGAAGATATACAAACAAATGCGGA-3′) and exon 7 (Aiol-ex7R, 5′-AGAGAGGCCTGTGTGAGAAGGCAC-3′) for 35 cycles (94°C for 30 seconds, 55°C for 30 seconds, and 72°C for 1 minute) in a final volume of 25 μl containing 1× PCR buffer (Gibco-BRL), 1.5 mM $MgCl_2$, 0.3 mM dNTP, 0.25 mM of each primer and 2 IU Taq polymerase (Gibco-BRL). GAPDH was used as an internal control to ensure cDNA quality and loading accuracy. Amplification products were resolved by agarose gel electrophoresis and visualized by ethidium bromide staining.

DNA hybridization

PCR products were blotted onto nylon membranes (Hybond-N+, Amersham Biosciences) and hybridized with a specific probe to confirm the specificity of amplification. DNA was cross-linked to the membrane by exposure to UV light. Membranes were prehybridized for 30 minutes and hybridized with an Aiolos probe, corresponding to a common region of all Aiolos isoforms and labeled with [α-^{32}P]dATP, for 5-6 hours. Membranes were then washed and exposed using high-sensitivity autoradiographic films with an intensifying screen (Agfa).

Isolation, cloning and sequencing of Aiolos isoforms

PCR products were separated by electrophoresis in TBE agarose gels and isolated from them using a SephaGlass BandPrep kit (Amersham Biosciences). The purified products were TA-cloned into the pGEM-T Easy Vector System (Promega) and sequenced in an ABI373 DNA sequencer (Applied Biosystems). The new isoforms were submitted to the GeneBank database, where they are listed under the following accession numbers: AY377973, AY377975, AY377976, AY377977, AY377978, AY377979, AY377980, AY377981 and AY377982.

The start codon of Aio-1, Aio-5a, Aio-Δ5, Aio-Δ3,4,5 and Aio-Δ3,4,5,6 cDNAs was replaced with a *Not*I restriction site by PCR mutagenesis using a specific primer (5′-GCGGCCGCGGAAGATATACAAACAAA-3′). This restriction site was used to tag a FLAG epitope at the 5′ end of the sequences maintaining the open reading frame of the transcripts. Constructions were subcloned into pCDNA3 vector at the *Not*I site for expression studies. All constructs were verified by DNA sequencing.

Immunoprecipitation and western blot analysis

FLAG-tagged Aio-1, Aio-5a, Aio-Δ5, Aio-Δ3,4,5 and Aio-Δ3,4,5,6 subcloned in pCDNA3-FLAG vector were transiently transfected with Lipofectamine-2000 (Invitrogen) into COS-7, which do not express Aiolos, following standard procedures. Cells were lysed with 1 ml of lysis buffer (50 mM Tris HCl, pH 7.4, 150 mM NaCl, 1 mM EDTA, 1% Triton X-100) and Complete EDTA-free (Roche) and FLAG-tagged proteins were immunoprecipitated with a mouse monoclonal anti-FLAG antibody (Sigma). Samples were loaded onto 10-12% SDS-polyacrylamide gels and electroblotted onto polyvinylidene difluoride (PVDF) membranes (Hybond-P, Amersham Biosciences). Immunodetection was performed with the following primary antibodies diluted in blocking solution (TBS-T-1% BSA): Anti-HDAC1 (ABR), anti-MTA1 (Abcam), Anti-MTA2 antibody (Abcam), Anti-MTA3 antibody (Abcam), Anti-SIN3A (Upstate), anti-Ikaros (M-20) (Santa Cruz Biotechnology), anti-FLAG antibody (Sigma). A rabbit polyclonal anti-Aiolos antiserum was made against a linear peptide corresponding to amino acids 5-18 of human Aiolos (QTNAELKSTQEQSVP). This antiserum recognizes all Aiolos isoforms. The secondary antibodies used were goat anti-rabbit conjugated to horseradish peroxidase (Amersham Biosciences) and sheep anti-mouse horseradish peroxidase (Amersham Biosciences). Blots were developed with the ECL Blotting Detection System (Amersham Biosciences).

Staining with fluorescent DNA probes and fluorescence microscopy

pCDNA3-FLAG-tagged Aiolos proteins were transiently transfected into cells previously plated overnight under poly-L-lysine-coated glass coverslips (10^6 cells/well for a six-well plate). Cells were fixed in 4% formaldehyde for 30 minutes at room temperature and permeabilized with phosphate-buffered saline-0.5% Triton X-100 for 10 minutes at room temperature. Staining with different antibodies, diluted in PBS buffer with 1% fetal bovine serum to block the non-specific antibody binding sites, was performed: Anti-HDAC1 (ABR), Anti-MTA2 antibody (Abcam), anti-SIN3A (Upstate), anti-Ikaros (M-20) (Santa Cruz Biotechnology), and anti-FLAG antibody (Sigma). Secondary antibodies used included anti-mouse IgG Cy3 conjugate and anti-rabbit IgG Cy2 conjugate (Jackson ImmunoResearch). DAPI (Dako) was used to stain the nucleus. Confocal optical sections were obtained using a Leica TCS SP confocal microscope (Leica Microsystems, Heidelberg GMbH) equipped with krypton and argon lasers, and images were processed using Adobe Photoshop 6.0 (Adobe Systems Inc.).

Isolation and western blotting of histones

Histones were acid-extracted from cell pellets in 0.25 M HCl and then acetone-precipitated (Fraga et al., 2005). Samples were separated on a 15% SDS-PAGE gel and blotted onto a 22-μm pore PVDF membrane (Immobilon PSQ; Millipore). The following rabbit polyclonal antibodies were used: anti-histone H3 (Abcam) directed against a C-terminal peptide of H3, anti-acetyl histone H3 (Upstate Biotechnologies, Inc.), anti-acetyl K9 histone H3 (Abcam), anti-histone H4 (Upstate Biotechnologies, Inc.), anti-acetyl histone H4 (Upstate Biotechnologies, Inc.), anti-acetyl K8 histone H4 (Abcam), and anti-acetyl K16 histone H4 (Upstate Biotechnologies, Inc.). Secondary antibodies used include anti-mouse and anti-rabbit IgG horseradish peroxidase conjugates (Amersham Biosciences) developed using ECL immunodetection reagents (Amersham Biosciences).

Quantification of global histone acetylation by high-performance capillary electrophoresis

The degree of histone acetylation was quantified by a modification of a previously described method (Fraga et al., 2005). Individual histones were fractionated by reversed-phase high-performance liquid chromatography (HPLC) on a Delta-Pak

C18 column (Waters) eluted with an acetonitrile gradient (20–60%) in 0.3% trifluoroacetic acid using a Beckman HPLC gradient system. Purity of histones was measured by PAGE. The non-, mono-, di-, tri- and tetraacetylated histone derivatives of H3 fraction were resolved by high-performance capillary electrophoresis (HPCE). An uncoated fused silica capillary (Beckman-Coulter; 60.2 cm × 75.0 mm, effective length 50.0 cm) was used in a CE system (P/ACETM MDQ; Beckman-Coulter) connected to a data-processing station (32 KaratTM Software). The running buffer was 110 mM phosphate buffer, pH 2.0, containing 0.03% (w/v) hydroxylpropylmethyl-cellulose. Running conditions were 25°C and an operating voltage of 12 kV. On-column absorbance was monitored at 214 nm. Before each run, the capillary system was conditioned by washing with 0.1 M NaOH for 3 minutes and 0.5 M H_2SO_4 for 2 minutes and equilibrated with the running buffer for 3 minutes. Samples were injected under pressure (0.3 psi) for 3 seconds. Triplicate samples were obtained and all samples were analyzed twice. Error bars in graphs represent standard deviations. Student's *t*-test was used to compare acetylation values (a P value <0.05 was considered to be statistically significant).

Chromatin immunoprecipitation (ChIP) assays

Standard ChIP assays were performed as previously described (Ballestar et al., 2003) using the anti-FLAG antibody and anti-Aiolos antiserum described above. In addition, a polyclonal antibody against RNA polymerase II (Abcam) was used as a positive control. Cell lysates were sonicated for 20 minutes with 30-second on-and-off cycles at the high setting of a Bioruptor (Diagenode) to produce chromatin fragments of 0.5 kb on average. At least three independent ChIP experiments were performed. PCR amplification was performed with specific primers for each of the analyzed promoters. For each promoter, the sensitivity of PCR amplification was evaluated in serial dilutions of total DNA collected after sonication (input fraction). Primer sequences to amplify the SIRT1 promoter are located around 300 bp upstream of the transcription start site and contain a consensus DNA binding site for Aiolos (TGGGAAA). The primers sequences are: forward SIRT1, TGCACGTGAGAAAACTGAGG and reverse SIRT1, GCTCCCTGAAATACGTTGGA. The promoter of the actin B gene was used as a control. Primer sequences, located at both sides of the transcription start site were: forward ACTB, CTCAATCTCGCTCTCGCTCT and reverse ACTB, CAAAGGCGAGGCTCTGTG. The criteria used to establish a positive result of Aiolos association were based on: (1) conditions of amplification in the linear range were optimized by PCR amplification of serial dilutions of total DNA collected after sonication (input fraction); (2) negative controls (no antibody) and input were included for each PCR experiment; (3) a minimum of three independent ChIP experiments were performed.

This work was supported by grants BFU2004-02073/BMC, CSD2006-49 and PM 99-0070 from the Spanish Ministry of Education and Science (MEC) and Mutua Madrileña Foundation. R.C. was funded by a Predoctoral Fellowship from the Spanish Ministry of Education and Science (PM 99-0070).

References

Ballestar, E., Paz, M. F., Valle, L., Wei, S., Fraga, M. F., Espada, J., Cigudosa, J. C., Huang, T. H.-M. and Esteller, M. (2003). Methyl-CpG binding proteins identify novel sites of epigenetic inactivation in human cancer. *EMBO J.* **22**, 6335-6345.

Bowen, N. J., Fujita, N., Kajita, M. and Wade, P. A. (2004). Mi-2/NuRD: multiple complexes for many purposes. *Biochim. Biophys. Acta* **1677**, 52-57.

Brown, K. E., Guest, S. S., Smale, S. T., Hahm, K., Merkenschlager, M. and Fisher, A. G. (1997). Association of transcriptionally silent genes with Ikaros complexes at centromeric heterochromatin. *Cell* **91**, 845-854.

Cobb, B. S., Morales-Alcelay, S., Kleiger, G., Brown, K. E., Fisher, A. G. and Smale, S. T. (2000). Targeting of Ikaros to pericentromeric heterochromatin by direct DNA binding. *Genes Dev.* **14**, 2146-2160.

Cokol, M., Nair, R. and Rost, B. (2000). Finding nuclear localization signals. *EMBO J.* **1**, 411-415.

Cortes, M. and Georgopoulos, K. (2004). Aiolos is required for the generation of high affinity bone marrow plasma cells responsible for long-term immunity. *J. Exp. Med.* **199**, 209-219.

Cortes, M., Wong, E., Koipally, J. and Georgopoulos, K. (1999). Control of lymphocyte development by the Ikaros gene family. *Curr. Opin. Immunol.* **11**, 167-171.

Dovat, S., Ronni, T., Russell, D., Ferrini, R., Cobb, B. S. and Smale, S. T. (2002). A common mechanism for mitotic inactivation of C2H2 zinc finger DNA-binding domains. *Genes Dev.* **16**, 2985-2990.

Fisher, A. G. (2002). Cellular identity and lineage choice. *Nat. Rev. Immunol*. **2**, 977-982.

Fraga, M. F., Ballestar, E., Villar-Garea, A., Boix-Chornet, M., Espada, J., Schotta, G., Bonaldi, T., Haydon, C., Ropero, S., Petrie, K. et al. (2005). Loss of acetylated lysine 16 and trimethylated lysine 20 of histone H4 is a common hallmark of human cancer. *Nat. Genet*. **37**, 391-400.

Fujita, N., Jaye, D. L., Kajita, M., Geigerman, C., Moreno, C. S. and Wade, P. A. (2003). MTA3, a Mi-2/NuRD complex subunit, regulates an invasive growth pathway in breast cancer. *Cell* **113**, 207-219.

Fujita, N., Jaye, D. L., Geigerman, C., Akyildiz, A., Mooney, M. R., Boss, J. M. and Wade, P. A. (2004). MTA3 and the Mi-2/NuRD complex regulate cell fate during B lymphocyte differentiation. *Cell* **119**, 75-86.

Georgopoulos, K. (2002). Haematopoietic cell-fate decisions, chromatin regulation and ikaros. *Nat. Rev. Immunol.* **2**, 162-174.

Georgopoulos, K., Moore, D. D. and Derfler, B. (1992). Ikaros, an early lymphoid-specific transcription factor and a putative mediator for T cell commitment. *Science* **258**, 808-812.

Georgopoulos, K., Winandy, S. and Avitahl, N. (1997). The role of the Ikaros gene in lymphocyte development and homeostasis. *Annu. Rev. Immunol.* **15**, 55-176.

Hahm, K., Cobb, B. S., McCarty, A. S., Brown, K. E., Klug, C. A., Lee, R., Akashi, K., Weissman, I. L., Fisher, A. G. and Smale, S. T. (1998). Helios, a T cell-restricted Ikaros family member that quantitatively associates with Ikaros at centromeric heterochromatin. *Genes Dev.* **12**, 782-796.

Honma, Y., Kiyosawa, H., Mori, T., Oguri, A., Nikaido, T., Kanazawa, K., Tojo, M., Takeda, J., Tanno, Y., Yokoya, S. et al. (1999). Eos: a novel member of the Ikaros gene family expressed predominantly in the developing nervous system. *FEBS Lett.* **447**, 76-80.

Humphrey, G. W., Wang, Y., Russanova, V. R., Hirai, T., Qin, J., Nakatani, Y. and Howard, B. H. (2001). Stable histone deacetylase complexes distinguished by the presence of SANT domain proteins CoREST/kiaa0071 and Mta-L1. *J. Biol. Chem*. **276**, 6817-6824.

Kelley, C. M., Ikeda, T., Koipally, J., Avitahl, N., Wu, L., Georgopoulos, K. and Morgan, B. A. (1998). Helios, a novel dimerization partner of Ikaros expressed in the earliest hematopoietic progenitors. *Curr. Biol.* **8**, 508-515.

Kim, J., Sif, S., Jones, B., Jackson, A., Koipally, J., Heller, E., Winandy, S., Viel, A., Sawyer, A., Ikeda, T. et al. (1999). Ikaros DNA-binding proteins direct formation of chromatin remodeling complexes in lymphocytes. *Immunity* **10**, 345-355.

Klug, C. A., Morrison, S. J., Masek, M., Hahm, K., Smale, S. T. and Weissman, I. L. (1998). Hematopoietic stem cells and lymphoid progenitors express different Ikaros isoforms, and Ikaros is localized to heterochromatin in immature lymphocytes. *Proc. Natl. Acad. Sci. USA* **95**, 657-662.

Koipally, J. and Georgopoulos, K. (2002a). A molecular dissection of the repression circuitry of Ikaros. *J. Biol. Chem.* **277**, 27697-27705.

Koipally, J. and Georgopoulos, K. (2002b). Ikaros-CtIP interactions do not require C-terminal binding protein and participate in a deacetylase-independent mode of repression. *J. Biol. Chem.* **277**, 23143-23149.

Koipally, J., Renold, A., Kim, J. and Georgopoulos, K. (1999). Repression by Ikaros and Aiolos is mediated through histone deacetylase complexes. *EMBO J.* **18**, 3090-3100.

Lareau, L. F., Green, R. E., Bhatnagar, R. S. and Brenner, S. E. (2004). The evolving roles of alternative splicing. *Curr. Opin. Struct. Biol.* **14**, 273-282.

Liippo, J., Nera, K. P., Veistinen, E., Lähdesmäki, A., Postila, V., Kimby, E., Riikonen, P., Hammarström, L., Pelkonen, J. and Lassila, O. (2001). Both normal and leukemic B lymphocytes express multiple isoforms of the human Aiolos gene. *Eur. J. Immunol.* **31**, 3469-3474.

Molnar, A. and Georgopoulos, K. (1994). The Ikaros gene encodes a family of functionally diverse zinc finger DNA-binding proteins. *Mol. Cell. Biol.* **14**, 8292-8303.

Morgan, B., Sun, L., Avitahl, N., Andrikopoulos, K., Ikeda, T., Gonzales, E., Wu, P., Neben, S. and Georgopoulos, K. (1997). Aiolos, a lymphoid restricted transcription factor that interacts with Ikaros to regulate lymphocyte differentiation. *EMBO J*. **16**, 2004-2013.

Nakase, K., Ishimaru, F., Fujii, K., Tabayashi, T., Kozuka, T., Sezaki, N., Matsuo, Y. and Harada, M. (2002). Overexpression of novel short isoforms of Helios in a patient with T-cell acute lymphoblastic leukemia. *Exp. Hematol*. **30**, 313-317.

Orlando, V. (2000). Mapping chromosomal proteins in vivo by formaldehyde-crosslinked-chromatin immunoprecipitation. *Trends Biochem. Sci.* **25**, 99-104.

Payne, K. J., Nicolas, J. H., Zhu, J. Y., Barsky, L. W. and Crooks, G. M. (2001). Cutting edge: predominant expression of a novel Ikaros isoform in normal human hemopoiesis. *J. Immunol*. **167**, 1867-1870.

Perdomo, J., Holmes, M., Chong, B. and Crossley, M. (2000). Eos and pegasus, two members of the Ikaros family of proteins with distinct DNA binding activities. *J. Biol. Chem.* **275**, 38347-38354.

Rebollo, A., Ayllon, V., Fleischer, A., Martinez, C. A. and Zaballos, A. (2001). The association of Aiolos transcription factor and Bcl-xL is involved in the control of apoptosis. *J. Immunol.* **167**, 6366-6373.

Romero, F., Martinez, A. C., Camonis, J. and Rebollo, A. (1999). Aiolos transcription factor controls cell death in T cells by regulating Bcl-2 expression and its cellular localization. *EMBO J.* **18**, 3419-3430.

Schmitt, C., Tonnelle, C., Dalloul, A., Chabannon, C., Debre, P. and Rebollo, A. (2002). Aiolos and Ikaros: regulators of lymphocyte development, homeostasis and lymphoproliferation. *Apoptosis* **7**, 277-284.

Sun, J., Matthias, G., Mihatsch, M. J., Georgopoulos, K. and Matthias, P. (2003). Lack of the transcriptional coactivator OBF-1 prevents the development of systemic lupus erythematosus-like phenotypes in Aiolos mutant mice. *J. Immunol.* **170**, 1699-1706.

Sun, L., Liu, A. and Georgopoulos, K. (1996). Zinc finger-mediated protein interactions modulate Ikaros activity, a molecular control of lymphocyte development. *EMBO J.* **15**, 5358-5369.

Sun, L., Goodman, P. A., Wood, C. M., Crotty, M.-L., Sensel, M., Sather, H., Navara, C., Nachman, J., Steinherz, P. G., Gaynon, P. S. et al. (1999). Expression of aberrantly spliced oncogenic Ikaros isoforms in childhood acute lymphoblastic leukemia. *J. Clin. Oncol.* **17**, 3753-3766.

Vaquero, A., Scher, M., Lee, D., Erdjument-Bromage, H., Tempst, P. and Reinberg, D. (2004). Human SirT1 interacts with histone H1 and promotes formation of facultative heterochromatin. *Mol. Cell* **16**, 93-105.

Wang, J. H., Avitahl, N. A., Cariappa, C., Friedrich, T., Ikeda, A., Renold, K. Andrikopoulos, L., Liang, S., Pillai, B. A., Morgan, B. A. et al. (1998). Aiolos regulates B cell activation and maturation to effector state. *Immunity* **9**, 543-553.

Yang, W. M., Tsai, S. C., Wen, Y. D., Fejer, G. and Seto, E. (2002). Functional domains of histone deacetylase-3. *J. Biol. Chem.* **277**, 9447-9454.